Dynamic RF Charging of Zero-Energy Devices via Reconfigurable Intelligent Surfaces

Morteza Tavana, *Student Member, IEEE*, Meysam Masoudi, and Emil Björnson, *Fellow, IEEE*

***Abstract*—Communication networks can achieve self-sustainability with the help of reconfigurable intelligent surfaces (RIS) that direct electromagnetic waves toward zero-energy devices (ZEDs) for energy harvesting. The harvested energy charges the ZEDs' batteries, reduces their dependency on external energy sources and enables energy neutrality. In this letter, we propose a dynamic algorithm that adjusts the joint RIS and TX phases based on the battery levels to maximize a weighted-sum power metric favoring ZEDs with lower battery levels. The simulation results show that threshold-based weighting slightly underperforms compared to the weighting with optimal parameters while requiring less data exchange with the network entity manager.**

***Index Terms*—Analog beamforming, energy harvesting, phased array, reconfigurable intelligent surface, zero-energy devices.**

I. Introduction

FUTURE wireless networks are expected to provide the necessary infrastructure for larger data rates, higher energy efficiency, and a massive number of connected devices. In the coming years, there will be a transition from a few billion to tens of billions of devices that need connectivity [1]. At such a massive scale, it will be essential for connected sensors to be inexpensive and consume minimal energy. Therefore, extending the battery life for Internet of Things devices and progressing towards zero-energy device (ZED) communication are becoming increasingly important. ZEDs eliminate the need for battery replacement or manual charging since they harvest energy from their surroundings. This versatile feature is highly beneficial for a wide range of devices with diverse functionalities, such as sensors (providing data from readings and measurements), trackers (indicating the location of an object or living entity), or actuators (stimulating other machines to function) [2], [3].

ZEDs have the potential to bring about a significant decrease in costs and power requirements for operating and maintaining devices, enabling greater scalability. Gathering data from these devices can lead to increased productivity, reduced pollution, and enhanced lifestyles without additional energy resources. Furthermore, these battery-free devices offer environmental benefits and can be managed through straightforward and uncomplicated processes, from manufacturing to disposal, presenting an additional advantage [4].

In general, there exist two classes of radio frequency (RF) power transfer: Simultaneous wireless information and power transfer (SWIPT) [5] that is mainly designed for downlink data transmission, and wirelessly powered communication network (WPCN) [6], [7], [8] that can be used for both uplink and downlink. One of the challenges in RF charging of ZEDs is the large pathloss that limits the power transfer efficiency. The path losses over wireless channels are 60+ dB. However, the beamforming gain for a 100-element antenna array is around 20 dB. Therefore, techniques such as energy beamforming are insufficient to achieve efficient wireless power transfer [9].

Recently, with the emergence of reconfigurable intelligent surfaces (RISs), it becomes possible to control the wave propagation environment and guide the electromagnetic waves toward the receiver via smart reflections [10]. A RIS with a large surface can collect more ambient RF energy and beamform it towards ZEDs; the power gain grows quadratically with the surface area. Hence, we can utilize RIS to power ZEDs by passively beamforming signal energy (from dedicated power sources or ambient sources) toward these devices. In [11], a SWIPT system aided by a RIS is proposed. A RIS is deployed to assist a multiantenna access point to serve multiple information decoding and energy harvesting (EH) receivers. To enable zero-energy RIS in the absence of coordination with the ambient power source, an amplitude-based sequential optimization algorithm for EH with RIS is proposed in [12].

To the best of our knowledge, the problem of dynamic prioritization for simultaneous RF charging of multiple ZEDs via a RIS is missing in the literature. Therefore, in this letter, we consider the problem of dynamic simultaneous charging of ZEDs with the assistance of a RIS. The main contributions, as compared to the previous works, are:

- We propose a dynamic joint analog beamforming and RIS-assisted EH framework, and we formulate an optimization problem to maximize the weighted-sum power of selected ZEDs taking into account their battery levels.
- For the weighted-sum power maximization, we propose an efficient scalable algorithm to obtain a stationary solution with locally non-increasing behavior in all coordinate directions at the convergence point.
- We propose a class of parameterized weighting functions and find the optimal parameters that minimize the mean time-averaged failure rate (FR) of the ZEDs.

The remainder of this letter is organized as follows. Section II describes the system model and problem formulation. Section III describes the proposed algorithm for the phase configuration of the RIS. Performance evaluation and the

Manuscript received 11 May 2024; accepted 10 June 2024. Date of publication 12 June 2024; date of current version 9 August 2024. This work was supported by Digital Futures. The associate editor coordinating the review of this article and approving it for publication was F. Shu. *(Corresponding author: Morteza Tavana.)*

Morteza Tavana and Emil Björnson are with the School of Electrical Engineering and Computer Science, KTH Royal Institute of Technology, 16440 Stockholm, Sweden (e-mail: morteza2@kth.se; emilbjo@kth.se).

Meysam Masoudi is with the Global AI Accelerator Unit, Ericsson, 115 41 Stockholm, Sweden (e-mail: meysam.masoudi@ericsson.com).

Digital Object Identifier 10.1109/LWC.2024.3413629

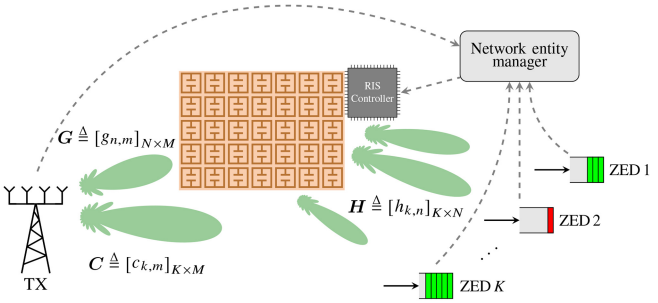

Fig. 1. Joint analog beamforming and RIS-assisted energy harvesting framework for ZEDs.

simulation results are presented in Section IV, while Section V provides our conclusions.

Notations: We denote the sets of non-negative integers and real numbers with $\mathbb{N}_0$ and $\mathbb{R}$, respectively. Vectors are indicated by lower-case bold-face letters, e.g., $\boldsymbol{x}$, and x_i (or $[x]_i$) denotes the ith element of $\boldsymbol{x}$. We represent matrices by upper-case bold-face letters, e.g., $\boldsymbol{A}$, and $[\boldsymbol{A}]_{m,n}$ indicates the element of $\boldsymbol{A}$ with row number m and column number n. We represent the conjugate of a complex number z with z^*. However, we denote the optimal solution with the superscript $\star$, e.g., $x^\star$. The operation $\mathrm{Arg}\,(z)$ returns the principal value of the argument of z that lies within the interval $(-\pi, \pi]$. The indicator function and Dirac delta function are denoted by $\mathbb{1}(\cdot)$ and $\delta(\cdot)$, respectively.

II. System Model and Problem Formulation

We consider the problem of charging of ZEDs with the assistance of a RIS. The setup is illustrated in Fig. 1. We aim to dynamically control the RIS phase configuration and the analog beamforming of the transmitter (TX) to facilitate battery charging for ZEDs. In this scenario, there is a M-antenna TX with power P_t and a RIS with N elements that assists the charging of K ZEDs. Each ZED is equipped with a small battery (or capacitor) to store energy for its future usage. Also, a network entity manager (NEM) communicates with different entities (e.g., RIS, TX, and ZEDs) and provides the necessary inputs to the RIS controller, such as the battery statuses of the ZEDs and the channel state information (CSI).[1]

The complex channel gain matrix between the TX and the ZED is represented as $\boldsymbol{C}$, where $[\boldsymbol{C}]_{m,k}$ is the complex channel gain between the TX antenna element m and the ZED k. Similarly, the complex channel gain matrix between the TX and the RIS elements is represented as $\boldsymbol{G}$, where $[\boldsymbol{G}]_{n,m}$ is the complex channel gain between the TX antenna element m and the RIS element n. We further assume that the complex channel gain matrix between the RIS elements and ZEDs is denoted as $\boldsymbol{H}$, where $[\boldsymbol{H}]_{k,n}$ is the complex channel gain between the ZED k and the RIS element n.

For a RIS phase configuration of $\boldsymbol{\vartheta} = [\vartheta_1, \vartheta_2, \ldots, \vartheta_N]^\mathbf{T}$ and analog beamforming phases $\boldsymbol{\varphi} = [\varphi_1, \varphi_2, \ldots, \varphi_M]^\mathbf{T}$, the received RF power by ZED k is

$$\rho_k(\boldsymbol{\vartheta}, \boldsymbol{\varphi}) = \frac{P_\mathrm{t}}{M} \left| \sum_{m=1}^{M} \left([\boldsymbol{C}]_{k,m} + \sum_{n=1}^{N} z_{k,n,m} e^{j\vartheta_n} \right) e^{j\varphi_m} \right|^2, \quad (1)$$

where $z_{k,n,m} \triangleq [\boldsymbol{G}]_{n,m}[\boldsymbol{H}]_{k,n}$. Moreover, for each $1 \le k \le K$, we assume that the ZED k consumes an energy packet of size γ_k at the random time instances $\mathcal{T}_k \triangleq \{t_{k,1}, t_{k,2}, \ldots\}$. Thus, the battery state of the ZED k evolves as

$$\frac{d}{dt} b_k(t) = \eta(\rho_k(\boldsymbol{\vartheta}(t), \boldsymbol{\varphi}(t))) - \gamma_k \cdot \mathbb{1}(t \in \mathcal{T}_k) \cdot \mathbb{1}(b_k(t) \ge \gamma_k) \cdot \delta(t), \quad (2)$$

where $b_k(t)$ is the battery level at the time t and $\eta(\cdot)$ is the harvesting power function.

In this letter, we assume that failures occur when ZEDs cannot carry out their tasks due to insufficient energy in their batteries. More formally, the number of failures of the ZED k during the time interval $[t, s)$ is defined as

$$F_k(t, s) \triangleq \sum_{\tau \in \mathcal{T}_k \cap [t,s)} \mathbb{1}(b_k(\tau) < \gamma_k). \quad (3)$$

The FR is the number of packet failures of ZEDs during a time unit. To minimize the average FR, we should solve the following dynamic stochastic optimization problem:

$$\begin{aligned}
\underset{\{\boldsymbol{\vartheta}(t), \boldsymbol{\varphi}(t): t \ge 0\}}{\text{minimize}} \quad & \lim_{T\to\infty} \frac{1}{T} \sum_{k=1}^{K} \mathbb{E}(F_k(t, T+t)) && \text{(4a)}\\
\text{subject to} \quad & b_k(\cdot) \text{ evolves as (2) } \forall 1 \le k \le k, && \text{(4b)}\\
& \boldsymbol{\vartheta} : \mathbb{N}_0 \to [0, 2\pi)^N, && \text{(4c)}\\
& \boldsymbol{\varphi} : \mathbb{N}_0 \to [0, 2\pi)^M, && \text{(4d)}\\
& \mathcal{T}_k \text{ is a random process } \forall 1 \le k \le k. && \text{(4e)}
\end{aligned}$$

For a strict-sense stationary (SSS) arrival processes $\{\mathcal{T}_k\}_{k=1}^K$, the objective (4a) is the same at $t = t_1$ and $t = t_2$ if $b_k(t_1) = b_k(t_2)$ for all $1 \le k \le K$. Thus, the optimal phase configuration policies $\boldsymbol{\vartheta}$ and $\boldsymbol{\varphi}$ are time-independent, and they depend on the battery level vector $\boldsymbol{b} \triangleq [b_1, b_2, \ldots, b_K]^\mathbf{T}$ that is the dynamic state variable of the problem. Thus, we drop the time index t and consider a time-independent policy for the RIS phase configuration. Dealing with discontinuous functions with dynamic state variables in the continuous time domain is challenging. However, the expected FR of each ZED k decreases with increasing the received power $\rho_k(\boldsymbol{\vartheta}, \boldsymbol{\varphi})$. Therefore, we consider an alternative problem formulation. For a scenario with multiple ZEDs (i.e., $K > 1$), we face the following multi-objective optimization problem (MOOP):

$$\underset{\boldsymbol{\vartheta} \in [0,2\pi)^N, \boldsymbol{\varphi} \in [0,2\pi)^M}{\text{maximize}} \; [\rho_1(\boldsymbol{\vartheta}, \boldsymbol{\varphi}), \ldots, \rho_K(\boldsymbol{\vartheta}, \boldsymbol{\varphi})]^\mathbf{T}. \quad (5)$$

In this MOOP, we aim to simultaneously maximize the received power by each ZED. In general, there is no globally optimal solution to (5) that maximizes all objectives simultaneously. Nevertheless, there are some prioritization techniques to deal with MOOPs. In our problem, depending on the battery statuses of the ZEDs, some of them will have higher priority to be powered than others. Hence, we will utilize these priorities to define a single-objective optimization problem.

[1] In a stationary environment with no moving objects, the channels remain static during the operation. Consequently, CSI can be obtained using the known positions of the entities or through channel estimation techniques.

The weighted sum is a common scalarization method to deal with MOOPs [13]. Therefore, we consider the weighted-sum power of the ZEDs as the objective function for the optimization problem. The weight vector is a non-negative function of the battery level vector. We assume $v : \mathbb{R}_+^K \to \mathbb{R}_+^K$ is a weight function that maps a battery level vector $\boldsymbol{b}$ to a weight vector $\boldsymbol{w} \triangleq [w_1, w_2, \ldots, w_K]^\top$. The optimization problem can be defined as

$$\underset{\boldsymbol{\vartheta}\in[0,2\pi)^N, \boldsymbol{\varphi}\in[0,2\pi)^M}{\text{maximize}} \quad f(\boldsymbol{\vartheta}, \boldsymbol{\varphi}), \tag{6}$$

where $f(\boldsymbol{\vartheta}, \boldsymbol{\varphi}) \triangleq \sum_{k=1}^K w_k \rho_k(\boldsymbol{\vartheta}, \boldsymbol{\varphi})$ with $\boldsymbol{w} \triangleq v(\boldsymbol{b})$.[2]

III. Proposed Solution

In this section, we propose a novel algorithm to address the weighted-sum power maximization problem, and we propose a dynamic scheme for RIS phase configuration based on the battery statuses of the ZEDs.

A. Weighted-Sum Power Maximization

The optimization problem (6) is non-convex and for $K > 1$, there is no closed-form solution for it. We propose an element-wise adjustment of the phase shifts of the RIS.

Consider the maximization of the weighted-sum power with respect to a single variable. We have the following lemma.

Lemma 1: Assuming $\tilde{f}(x) \triangleq \sum_{k=1}^K w_k |a_k + b_k e^{jx}|^2$, the value of x that maximizes $\tilde{f}(\cdot)$ is $x^\star \triangleq \text{Arg}\left(\sum_{k=1}^K w_k a_k b_k^*\right)$.

Proof: We have

$$\begin{aligned} x^\star &= \underset{x}{\text{argmax}} \sum_{k=1}^K w_k \left(|a_k|^2 + |b_k|^2 + 2\,\text{Re}\left(a_k b_k^* e^{-jx}\right)\right) \\ &= \underset{x}{\text{argmax}}\ \text{Re}\left(e^{-jx} \sum_{k=1}^K w_k a_k b_k^*\right) = \text{Arg}\left(\sum_{k=1}^K w_k a_k b_k^*\right). \end{aligned} \tag{7}$$

■

To maximize the weighted-sum power with respect to all variables, we propose Algorithm 1, which is a sequential algorithm developed based on Lemma 1. The method initializes the RIS phase vector and the TX precoder with random phases. Afterwards, it updates the phase of the first element of the RIS using (7). Then, it proceeds to the next element and follows the same procedure until the algorithm applies the phase updates to all elements of the RIS. Similarly, the algorithm updates the phases of the precoder based on Lemma 1.[3] The process is repeated to reach a convergence accuracy of $\varepsilon > 0$. This means that the ratio between the weighted-sum power in the last iteration and the one in the previous iteration is less than $1 + \varepsilon$.[4]

[2]The proposed optimization problem does not incorporate the nonlinear harvesting power function as it makes the problem mathematically intractable.

[3]We skip updating the phase of the first element since a constant phase shift of all elements in the precoder vector does not affect the objective function.

[4]Algorithm 1 can be implemented in a more computationally efficient way by defining $s \triangleq \sum_{m=1}^M ([\boldsymbol{C}]_{k,m} + \sum_{n=1}^N z_{k,n,m} e^{j\vartheta_n}) e^{j\varphi_m}$ before the while loop and modifying its value after each elementwise phase update. Additionally, we can update $e^{j\vartheta_n}$ and $e^{j\varphi_m}$ rather than ϑ_n and φ_m in the phase update of each RIS element n and TX element m, which makes the algorithm run even faster. However, for the sake of clarity, we didn't include these refinements in Algorithm 1.

Algorithm 1: Weighted-Sum Power Maximization

Input: The number of RIS elements N, the number of TX antenna elements M, convergence accuracy $\varepsilon > 0$, weights $\{w_k\}_{k=1}^K$, $\boldsymbol{C}$, $\boldsymbol{G}$, and $\boldsymbol{H}$.
Output: The stationary phase vector $\boldsymbol{\vartheta}^\star$ and $\boldsymbol{\varphi}^\star$.
Initialize: $\boldsymbol{\vartheta}$ and $\boldsymbol{\varphi} \leftarrow$ randominitialvectors, and $f_{\text{old}} \leftarrow 0^+$.
while $f(\boldsymbol{\vartheta}, \boldsymbol{\varphi})/f_{\text{old}} - 1 > \varepsilon$ **do**
  $f_{\text{old}} \leftarrow f(\boldsymbol{\vartheta}, \boldsymbol{\varphi})$;
  for $n \leftarrow 1$ **to** N **do**
    $\boldsymbol{a} \leftarrow [0, \ldots, 0]^{\mathbf{T}}$;
    for $k \leftarrow 1$ **to** K **do**
      $a_k \leftarrow \sum_{m=1}^M \left([\boldsymbol{C}]_{k,m} + \sum_{\substack{i=1 \\ i\neq n}}^N z_{k,i,m} e^{j\vartheta_i}\right) e^{j\varphi_m}$;
    end
    $\vartheta_n \leftarrow \text{Arg}\left(\sum_{k=1}^K w_k a_k \sum_{m=1}^M z_{k,n,m}^* e^{-j\varphi_m}\right)$;
  end
  for $m \leftarrow 2$ **to** M **do**
    $\boldsymbol{a} \leftarrow [0, \ldots, 0]^{\mathbf{T}}$;
    for $k \leftarrow 1$ **to** K **do**
      $a_k \leftarrow \sum_{\substack{i=1 \\ i\neq m}}^M \left([\boldsymbol{C}]_{k,i} + \sum_{n=1}^N z_{k,n,i} e^{j\vartheta_n}\right) e^{j\varphi_i}$;
    end
    $\varphi_m \leftarrow \text{Arg}\left(\sum_{k=1}^K w_k a_k \left([\boldsymbol{C}]_{k,m}^* + \sum_{n=1}^N z_{k,n,m}^* e^{-j\vartheta_n}\right)\right)$;
  end
end
$\boldsymbol{\vartheta}^\star \leftarrow \boldsymbol{\vartheta}$;
$\boldsymbol{\varphi}^\star \leftarrow \boldsymbol{\varphi}$;

Theorem 1: For a small enough $\varepsilon > 0$, the proposed Algorithm 1 converges to a stationary point with locally non-increasing behavior in all coordinate directions of (6).

Proof: Since Algorithm 1 sequentially maximizes the function f for the phase of each element based on Lemma 1, it produces a monotonically non-decreasing sequence. Given that f has finite upper bounds, the algorithm converges to a finite value according to the monotone convergence theorem [14]. From (7), at the point of convergence, $\nabla f(\boldsymbol{\vartheta}^\star, \boldsymbol{\varphi}^\star) = \mathbf{0}$. Moreover, for each n and m, $\partial^2 f(\boldsymbol{\vartheta}^\star, \boldsymbol{\varphi})/\partial\vartheta_n^2 \leq 0$ and $\partial^2 f(\boldsymbol{\vartheta}, \boldsymbol{\varphi}^\star)/\partial\varphi_m^2 \leq 0$, indicating that in the neighborhood of $\boldsymbol{\vartheta}^\star$, the function f exhibits locally non-increasing behavior in all coordinate directions. ■

B. Dynamic Phase Configuration

In a dynamic scenario, the RIS controller periodically receives the battery statuses and the identity indices of the ZEDs,[5] and generates the corresponding weights. Then, it dynamically updates the phase configuration of the RIS according to Algorithm 2.

[5]If a battery state hasn't changed in a specific period, no update needs to be sent.

Algorithm 2: Dynamic RIS and TX Phase Updates

Input: The number of RIS elements N, the number of TX antenna elements M, convergence accuracy $\varepsilon > 0$, weight function $v(\cdot)$, $\boldsymbol{C}$, $\boldsymbol{G}$, and $\boldsymbol{H}$.
Output: The dynamic phase vectors $\boldsymbol{\vartheta}^\star$ and $\boldsymbol{\varphi}^\star$.
Initialize: $w_k \leftarrow 1$ for all $1 \leq k \leq k$.
while *true* **do**
  if *any update on the battery statuses* **then**
    $\boldsymbol{w} \leftarrow v(\boldsymbol{b})$;
    $(\boldsymbol{\vartheta}^\star, \boldsymbol{\varphi}^\star) \leftarrow$ outputofAlgorithm 1;
  end
end

In general, the weights should be higher for the ZEDs with lower battery levels. Below, we introduce a class of weight functions $\nu_{\alpha,\beta}(\cdot)$ with parameters, α and β, as follows:

$$w_k = \left[\nu_{\alpha,\beta}(\boldsymbol{b})\right]_k \triangleq \frac{b_k^{-\alpha} \cdot \mathbb{1}(b_k \leq \beta) + \prod_{l=1}^{K} \mathbb{1}(b_l > \beta)}{\sum_{k'=1}^{K} \left(b_{k'}^{-\alpha} \cdot \mathbb{1}(b_{k'} \leq \beta) + \prod_{l=1}^{K} \mathbb{1}(b_l > \beta) \right)}, \quad (8)$$

where the denominator is simply for scaling and does not affect the solution for finite values of α. The following weight functions that we will compare in the performance evaluation are specific cases of (8).

1) Max-Min weighting: In max-min weighting, the goal is to maximize the received power of the ZED with the lowest battery level. This is a specific case of (8) assuming $\alpha \to \infty$ and $\beta \to \infty$. Note that the lowest battery level is a dynamic status, not fixed to any specific ZED. To generate the max-min weights, the algorithm needs to have all battery levels.

2) Threshold-Based weighting: This method maximizes the sum received power of ZEDs with battery levels below a threshold β, which is a specific case of (8) with $\alpha = 0$. Some ZEDs may have significantly stronger channels compared to others, resulting in sufficient power reception to charge their batteries regardless of the RIS phase configuration. Threshold-based weighting can eliminate their impact on the objective function and simplify that by removing terms related to ZEDs with a weight of zero. Additionally, the system can be designed such that the ZEDs communicate only binary data with the NEM when their batteries fall below the specified threshold.

IV. Performance Evaluation

In this section, we demonstrate the impact of using analog beamforming and RISs in reducing the FR in a dynamic remote charging scenario. We consider a TX with $M = 8$ antenna elements, a RIS with $N = 20$ elements, and $K = 10$ ZEDs in its surroundings. We consider independent and identically distributed (i.i.d.) Rayleigh fading channels, where $\sigma_G = 0.2$, $\sigma_H = 0.1$, and $\sigma_C = 0.01$. Additionally, we assume that the energy packet departure from the ZEDs follows a Poisson process with parameter $\lambda = 0.5$, and the corresponding energy consumption per packet is 70 mJ. The transmit power is $P_{\mathrm{t}} = 1$ W, the battery capacity of each ZED is 1 J, and the batteries are empty at the beginning of the simulation. Moreover, we consider a convergence accuracy of $\varepsilon = 10^{-4}$.

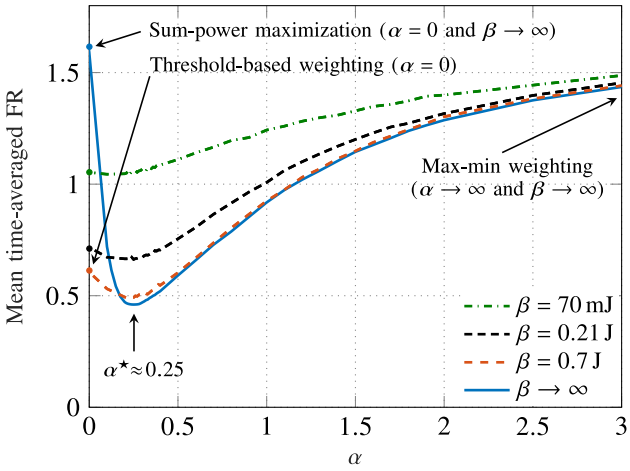

Fig. 2. Impact of weighting function parameters α and β on the mean time-averaged FR for $\eta(x) = 0.7\,x$.

We consider the following benchmark methods:

1) *Power method with random RIS phases:* We apply a modified power iteration method, as described in [15, Ch. 9], for analog beamforming at the TX. This approach is utilized in the presence of a RIS in the environment, with its elements having random phases.
2) *Sum-power maximization:* This method maximizes the sum of the received powers at ZEDs, as detailed in [11].

For a given weight function, in each simulation run, the time-averaged FR is random due to the randomness of channel realizations and the stochastic nature of packet departure processes. To understand the impact of parameters in the general weight function definition in (8), we conducted the simulation 30000 times. This was done to obtain the mean time-averaged FR for various parameters of α and β, as illustrated in Fig. 2. We observe that the minimum mean time-averaged FR is achieved for the weighting function parameters $\alpha^\star \approx 0.25$ and $\beta \to \infty$.

For the proposed method, we consider the three ways of selecting the weights described in Section III-B:

1) *Max-min weighting*, where we maximize the received power of the ZED with the worst battery level.
2) *Threshold-based weighting*, where we maximize the received sum power of the ZEDs with battery levels below a threshold of 0.7 J.
3) *Weighting with optimal parameters*, where we maximize the weighted-sum power of the ZEDs with weights from (8), considering weighting parameters that minimize the mean time-averaged FR.

For the simulation, we define the time-varying moving average FR during a time window $[t, t + W)$ for some $W > 0$:

$$\mathbf{FR}_W(t) \triangleq \frac{1}{W} \sum_{k=1}^{K} F_k(t, t + W). \quad (9)$$

Fig. 3 shows the moving average FRs (over 100 s), i.e., $\mathbf{FR}_{100}(t)$ as defined in (9) for the different schemes, respectively. It is observed that the weighting with optimal parameters outperforms all other schemes. The runner-up is the threshold-based scheme that requires less data exchange with the NEM, making it more desirable in that regard.

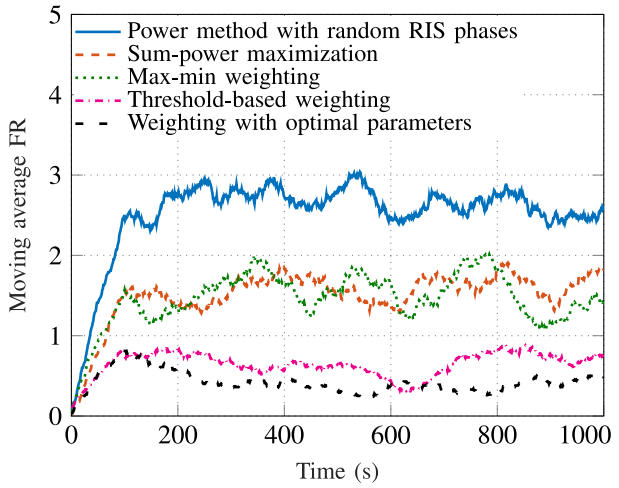

Fig. 3. The moving average FRs (over a time window of 100 s) for different schemes.

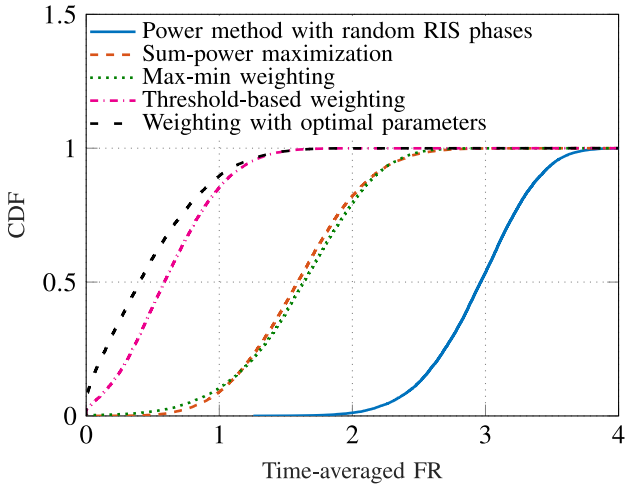

Fig. 4. CDF of the time-averaged FRs for different schemes (the randomness is related to the random channel realizations and stochastic packet departures).

In Fig. 4, we compared the CDF of the time-averaged FR across different schemes, where the randomness arises from the channel realizations and stochastic packet departure processes. As observed, the weighting with optimal parameters yields a lower FR compared to the other schemes.

The mean time-averaged FR is presented in Table I, providing a performance comparison for various schemes and both linear and nonlinear harvesting modules. For the linear scenario, we consider the harvesting efficiency function $\eta(x) = 0.7\,x$. For the nonlinear scenario, we use the sigmoidal function proposed in [16], and we have selected the parameters from previous work [12].

V. Conclusion

We have presented a mechanism to enable ZEDs through RIS-assisted energy harvesting in a scenario with dynamic traffic. By updating the TX and the RIS phase configurations based on the ZEDs' battery statuses, we effectively reduce the failure rate, that is, the risk that a device cannot conduct its designated task due to lack of energy. This letter concentrates on formulating the problem and developing optimization methods but also compares a few weighting techniques to obtain general design guidelines. However, future work could explore additional methods. Among the considered weighting schemes, the threshold-based approach slightly underperforms compared to the weighting with optimal parameters while requiring minimal data exchange with the NEM. This makes it a desirable choice for practical implementations.

TABLE I
Performance Comparison

Method	Mean time-averaged FR	
	Linear	Nonlinear
Power method with random RIS phases	2.94	3.51
Sum-power maximization	1.59	2.07
Max-min weighting	1.61	2.82
Threshold-based weighting	0.61	1.19
Weighting with optimal parameters	0.46	1.04

References

[1] S. Sinha, "State of the IoT 2023." May 2023. [Online]. Available: https://iot-analytics.com/number-connected-iot-devices/
[2] T. Zhang, M. Afshang, M. Mozaffari, and Y.-P. E. Wang, "Toward zero-energy devices: Waveform design for low-power receivers," *IEEE Commun. Lett.*, vol. 27, no. 8, pp. 2038–2042, Aug. 2023.
[3] S. Naser, L. Bariah, S. Muhaidat, and E. Basar, "Zero-energy devices empowered 6G networks: Opportunities, key technologies, and challenges," *IEEE Internet Things Mag.*, vol. 6, no. 3, pp. 44–50, Sep. 2023.
[4] S. Parkvall and T. Palacios, "Zero-energy devices—A new opportunity in 6G." 2021. [Online]. Available: https://www.ericsson.com/en/blog/2021/9/zero-energy-devices-opportunity-6g
[5] R. Zhang and C. K. Ho, "MIMO broadcasting for simultaneous wireless information and power transfer," *IEEE Trans. Wireless Commun.*, vol. 12, no. 5, pp. 1989–2001, May 2013.
[6] H. Ju and R. Zhang, "Throughput maximization in wireless powered communication networks," *IEEE Trans. Wireless Commun.*, vol. 13, no. 1, pp. 418–428, Jan. 2014.
[7] M. Tavana, M. Ozger, A. Baltaci, B. Schleicher, D. Schupke, and C. Cavdar, "Wireless power transfer for aircraft IoT applications: System design and measurements," *IEEE Internet Things J.*, vol. 8, no. 15, pp. 11834–11846, Aug. 2021.
[8] M. Tavana, E. Björnson, and J. Zander, "Range limits of energy harvesting from a base station for battery-less Internet-of-Things devices," in *Proc. IEEE Int. Conf. Commun. (ICC)*, 2022, pp. 153–158.
[9] R. Du, H. Shokri-Ghadikolaei, and C. Fischione, "Wirelessly-powered sensor networks: Power allocation for channel estimation and energy beamforming," *IEEE Trans. Wireless Commun.*, vol. 19, no. 5, pp. 2987–3002, May 2020.
[10] E. Björnson, H. Wymeersch, B. Matthiesen, P. Popovski, L. Sanguinetti and E. de Carvalho, "Reconfigurable intelligent surfaces: A signal processing perspective with wireless applications," *IEEE Signal Process. Mag.*, vol. 39, no. 2, pp. 135–158, Mar. 2022.
[11] Q. Wu and R. Zhang, "Weighted sum power maximization for intelligent reflecting surface aided SWIPT," *IEEE Wireless Commun. Lett.*, vol. 9, no. 5, pp. 586–590, May 2020.
[12] M. Tavana, M. Masoudi, and E. Björnson, "Energy harvesting Maximization for reconfigurable intelligent surfaces using amplitude measurements," *IEEE Trans. Commun.*, vol. 72, no. 4, pp. 2201–2215, Apr. 2024.
[13] C. Bazgan, S. Ruzika, C. Thielen, and D. Vanderpooten, "The power of the weighted sum scalarization for approximating multiobjective optimization problems," *Theory Comput. Syst.*, vol. 66, pp. 395–415, Feb. 2022.
[14] V. I. Bogachev and M. A. S. Ruas, *Measure Theory*, vol. 1. Berlin, Germany: Springer, 2007.
[15] E. Björnson and Ö. T. Demir, *Introduction to Multiple Antenna Communications and Reconfigurable Surfaces*. Norwell, MA, USA: Now Publ., Inc., 2024.
[16] E. Boshkovska, D. W. K. Ng, N. Zlatanov, and R. Schober, "Practical non-linear energy harvesting model and resource allocation for SWIPT systems," *IEEE Commun. Lett.*, vol. 19, no. 12, pp. 2082–2085, Dec. 2015.